What triggers Koyna region earthquakes? Preliminary results from seismic tomography digital array

S S Rai, Sunil K Singh, P V S S Rajagopal Sarma, D Srinagesh, K N S Reddy, K S Prakasam and Y Satyanarayana

National Geophysical Research Institute, Uppal Road, Hyderabad 500 007, India

The cause for prolific seismicity in the Koyna region is a geological enigma. Attempts have been made to link occurrence of these earthquakes with tectonic strain as well as the nearby reservoirs. With a view to providing reliable seismological database for studying the earth structure and the earthquake process in the Koyna region, a state of the art digital seismic network was deployed for twenty months during 1996–97. We present preliminary results from this experiment covering an area of $60\times80\,km^2$ with twenty seismic stations. Hypocentral locations of more than 400 earthquakes confined to $11\times25\,km^2$ reveal fragmentation in the seismicity pattern – a NE – SW segment has a dip towards NW at approximately 45°, whilst the other two segments show a near vertical trend. These seismic segments have a close linkage with the Western Ghat escarpment and the Warna fault. Ninety per cent of the seismicity is confined within the depth range of 3–10 km. The depth distribution of earthquakes delimits the seismogenic zone with its base at 10 km indicating a transition from an unstable to stable frictional sliding regime. The lack of shallow seismicity between 0 and 3 km indicates a mature fault system with well-developed gouge zones, which inhibit shallow earthquake nucleation. Local earthquake travel time inversion for P- and S-waves show ≈ 2% higher velocity in the seismogenic crust (0–10 km) beneath the epicentral tract relative to a lower velocity (2–3%) in the adjoining region. The high P- and S-wave velocity in the seismogenic crust argues against the presence of high pressure fluid zones and suggests its possible linkage with denser lithology. The zone of high velocity has been traced to deeper depths (≈ 70 km) through teleseismic tomography. The results reveal segmented and matured seismogenic fault systems in the Koyna region where seismicity is possibly controlled by strain build up due to competent lithology in the seismic zone with a deep crustal root.

1. Introduction

The Koyna Seismic Zone (KSZ, Gubin 1969) forming part of the Western Ghat in the south-western part of the Deccan volcanic province is a region of prolific seismicity. Our present knowledge about the seismicity of this region spans over three decades, during which over 100,000 earthquakes have been recorded. The record of seismicity prior to 1962 is very limited due to the absence of seismic stations in this area. During 1594 to 1832 between Bombay (18.8°N, 73°E) and Goa (15.5°N, 74°E) there were at least fifteen felt earthquakes (Gubin 1968; Kelkar 1968). The most destructive earthquake (magnitude 6.3) occurred in the Koyna region on December 10th, 1967 (Gupta *et al* 1969). Due to the proximity of the seismic zone to the reservoirs (Koyna and Warna) and the temporal association of seismic activity with their impoundments as well as the correlation with the changing water levels in them, Gupta (1992), Chadha *et al* (1997) and Talwani (1997) proposed a causal association between them. Lee and Raleigh (1969), however, argued in favour of tectonic strain as the cause for Koyna region seismicity. Gubin (1969) opined that the load due to the Koyna reservoir on traps, above the active fault was not the cause for seismicity. He favoured the view that continued development of the West Coast fault was due to the unequal uplift of

Keywords. Koyna; earthquake; digital seismograph; seismic tomography.

Proc. Indian Acad. Sci. (Earth Planet. Sci.), **108**, No. 1, March 1999, pp. 1–14

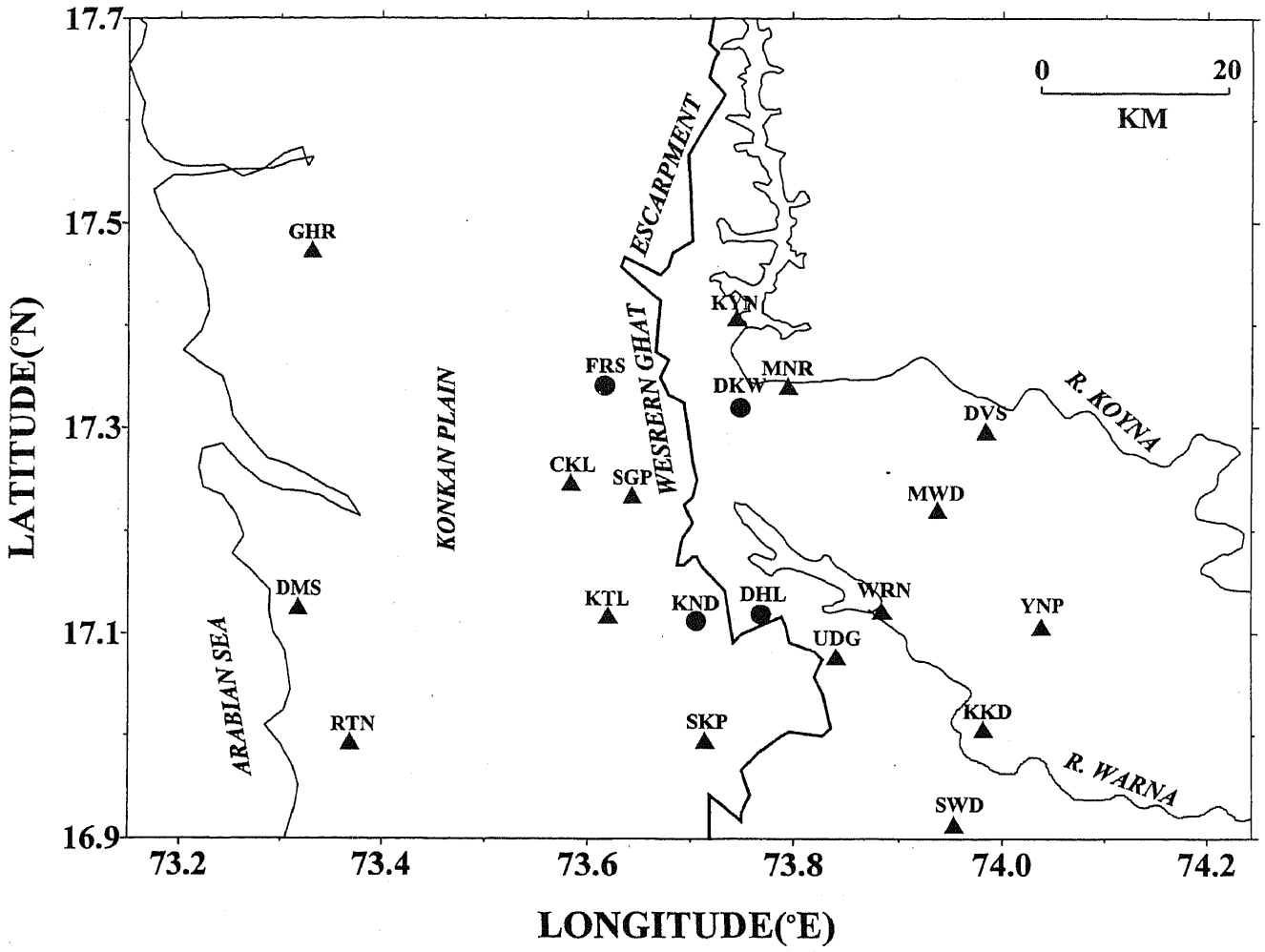

Figure 1. Major tectonic and geomorphic features of Koyna Seismic Zone alongwith location of seismic stations operated during the period April 1996–Dec 1997. Only data pertaining to stations shown by solid triangles were used for this study.

the western margin during the quaternary, which provided the causative source for strain accumulation.

The Koyna seismic zone in the Deccan volcanic province (figure 1) lies to the east of the west-facing escarpment about 50 km away from the Arabian Sea. The escarpment is a boundary between two regions of contrasting elevations. The region to the west marked by lower elevations ($\approx$ 100 to 200 m) is known as the "Konkan Plain" while the higher elevated (>1 km) Western Ghats lie to the east. The escarpment, a remarkable N-S linear feature runs parallel to the coast from the Gulf of Cambay to the Peninsular tip. Varied evolutionary mechanisms for this escarpment have been proposed. Some have suggested this to be a fault scarp (Pascoe 1964; Valdiya 1984) while others proposed it to be an erosional feature (Widdowson and Cox 1996). The region to the west of the scarp line has been grouped into a belt of active rifts and to the east as a platformal region by Mahadevan (1994) based on a synthesis of several data sources.

With a view to understanding the earthquake mechanism and dynamics of the KSZ, Seismic Tomography Program at the National Geophysical Research Institute embarked upon this research initiative supported by the Department of Science and Technology, to acquire high quality seismological data in the region. The seismological experiment focuses on:

- Imaging the active fault system(s).
- 3-D imaging of the seismogenic crust and uppermost mantle in terms of three distinct elastic wave parameters (V_P, V_S, Q).
- Study of the earthquake source parameters – earthquake rupture process(es), fault dimension, directivity effect, state of stress in the seismogenic layer.
- The study of the non-linear phenomena of earthquake clouds.

We present here the preliminary results obtained from the seismic tomography network in the KSZ based on observations for the period April 1996 to June 1997.

2. Seismicity

The nature of seismicity in the Koyna region can be categorised into different temporal phases: Prior to

1962: historical; 1962–1993: primitive analog instrumentation; 1993–1996: analog and digital instrumentation; 1996–1997: digital network. Information about historical seismicity (prior to 1962) is based on the compilations of Gubin (1968) and Kelkar (1968). Between 1594 and 1835, over fifteen earthquakes are reported to have occurred along the coastal strip between Bombay and Goa. Some of them were also felt in the vicinity of Koyna. In 1952 and 1962, earthquakes were felt in the coastal towns of Jaigarh (17.4°N, 72.3°E) and Ratnagiri (17°N, 72°E).

Intensity distribution of the 1967 Koyna earthquake exhibits a N-S trending irregular elliptical feature. Areas of intensities > 4 were elongated in a N-S direction parallel to the trend of the Western Ghat. Higher intensities (> 6) were clustered around the epicentral region, while the lower intensity isoseismals were wide apart. Such irregular patterns of intensities are usually associated with platformal earthquakes originating due to deep seated steep faults (Gubin 1969). Fault plane solutions and moment tensor inversion (Langston 1981; Langston and Franco-Spera 1985; Dziewonski *et al* 1988) of foreshocks, aftershocks and other events indicate strike slip to normal faulting in the region. Wide spread ground deformation had been observed along NNE-SSW, associated with the 1967 earthquake (GSI, 1968). Snow (1982) indicates the presence of a N-S trending fault with the west side down thrown.

Instrumental recording in the KSZ began in 1963, initially with four analog stations and subsequently increased to eight and eleven in 1973 and 1984 respectively, consisting of Wood-Anderson seismographs and smoke-drum recorders. Until 1984, all instruments had the manual option of impinging time thereby leading to significant error in hypocenter locations. Radio signals from BBC have been impinged on the seismogram since 1985. Subsequently in 1993, eight more seismographs (5 Portacorders and 3 Teledyne-Geotech's PDAS) were added to the existing network of eleven stations. Since these digital systems were not linked to any external timing devices like GPS, Omega clocks etc, there was no mechanism to correct for the drift in the systems' clocks, and therefore only S-P data were used for the location. Time synchronization with BBC signal leads to an error of 0.2 to 0.4 sec relative to GPS timings. Additionally, lower drum speed (60 mm/min, prior to 1993 and 120 mm/min afterwards) resulted in lower resolution, as the reading accuracy of P-onset is restricted to ≈ 0.2 sec. Talwani *et al* (1996) reanalysed data for 1963–95. Chadha *et al* (1997) and Mandal *et al* (1998) analysed data for 1993–95 and inferred two parallel NNE-SSW directed seismic trends with a left lateral strike slip movement. Due to poor control on the timing system, large inter-station separation with mostly vertical component recording and absence of stations in the near vicinity of the earthquake zone, focal depth errors are large and generally greater than 3 km. The errors in epicenter location vary between 2 and 3 km. This is demonstrated in a recent study by Talwani *et al* (1996). For the data set of 1993–95, no detailed error statistics have been provided by Chadha *et al* (1997) and Mandal *et al*

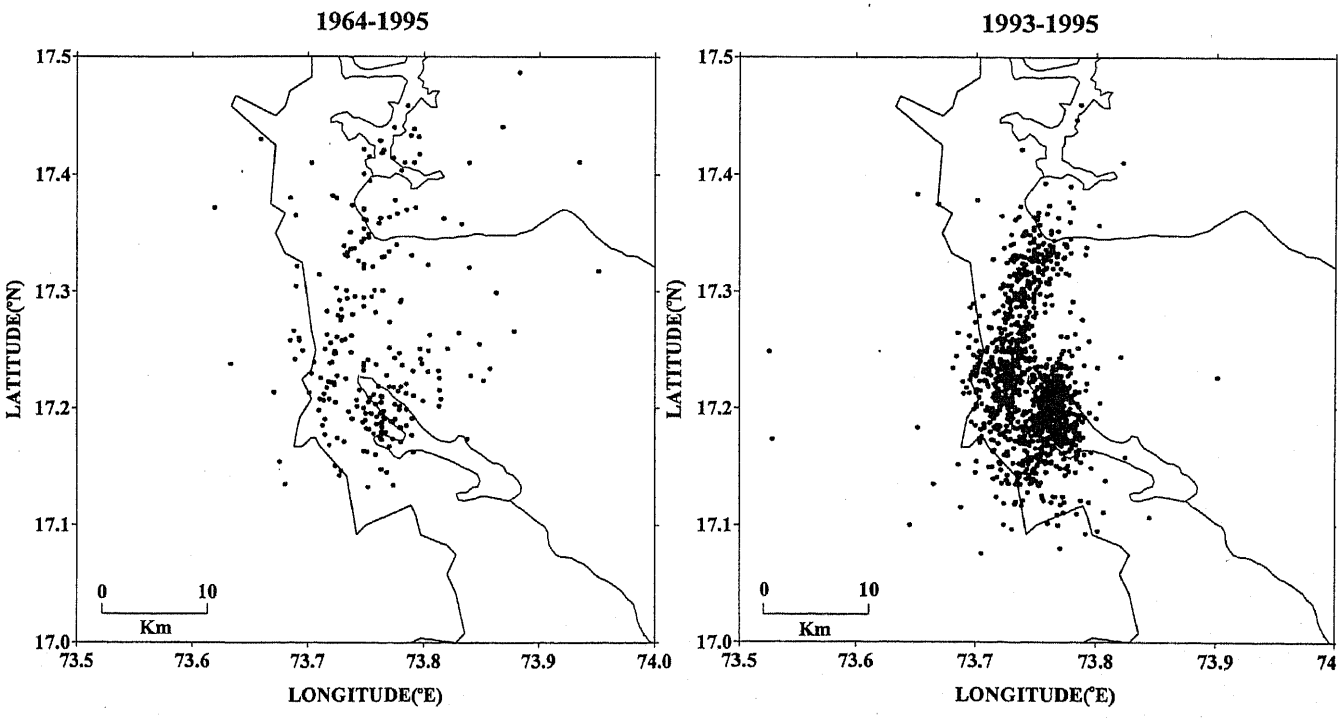

Figure 2. Epicenter locations from earlier studies: 1964–1995 (listed in Talwani *et al* 1996) and 1993–1995 (Chadha *et al* 1997; Mandal *et al* 1998). Magnitude range:- $2.3 \leq M_d \leq 5.4$ (1964–1995), $0.2 \leq M_d \leq 5.4$ (1993–1995).

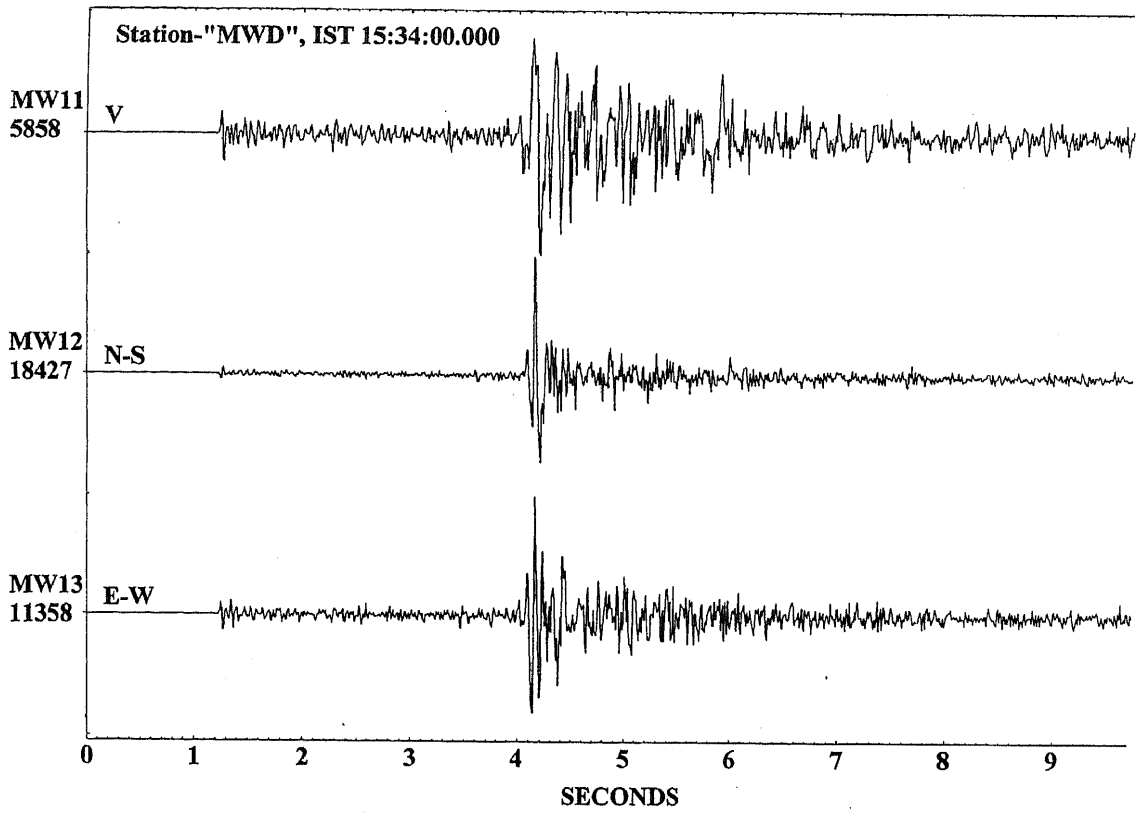

Figure 3. A typical earthquake recorded at station "MWD".

Table 1. *Location of seismic stations and the period of operation.*

Coordinates, elevations and period of operation for stations of Koyna digital network							
No.	Station	Latitude (°N)		Longitude (°E)		Elevation (m)	Period of Operation
		Degree	Min.	Degree	Min.		
1	MNR	17	20.51	73	47.73	533	22/4/96 to 06/01/98
2	DVS	17	17.84	73	59.07	560	22/4/96 to 17/11/96
3	YNP	17	06.45	74	02.26	638	22/4/96 to 22/01/97
4	KTL	17	07.11	73	37.19	110	22/4/96 to 15/02/97 27/6/97 to 20/10/97
5	SWD	16	54.84	73	57.21	500	22/4/96 to 25/05/97
6	SKP	16	59.76	73	42.88	230	22/4/96 to 17/09/97
7	SGP	17	14.09	73	38.66	240	22/4/96 to 05/01/98
8	WRN	17	07.39	73	53.07	560	22/4/96 to 19/05/97 01/7/97 to 07/01/98
9	MWD	17	13.27	73	56.27	610	22/4/96 to 06/01/98
10	KKD	17	00.43	73	58.91	504	20/5/97 to 15/09/97
11	CKL	17	14.82	73	35.08	90	22/4/96 to 05/01/98
12	FRS	17	20.53	73	37.01	100	27/9/97 to 05/01/98
13	UDG	17	04.69	73	50.43	860	30/5/97 to 21/10/97
14	DHL	17	07.18	73	46.13	825	21/10/97 to 04/1/98
15	DKW	17	19.21	73	44.94	565	20/10/97 to 06/1/98
16	RTN	16	59.66	73	22.17	107	27/11/96 to 27/6/97
17	DMS	17	07.59	73	19.09	118	15/2/97 to 30/06/97
18	GHR	17	28.46	73	19.90	113	04/2/97 to 29/06/97
19	KND	17	06.78	73	42.39	186	16/9/97 to 05/01/98
20	KYN	17	24.50	73	44.74	583	20/6/97 to 06/01/98

(1998). The epicentral location for earthquakes with A, B and C quality for 1964–95 (listed in Talwani *et al* 1996) and 1993–95 (Mandal *et al* 1998) are presented in figure 2.

3. Koyna seismic tomography digital network (1996–1997)

The Koyna seismic tomography digital network comprises of 24 bit REFTEK/PASSCAL (72A-07) recorders with a 500 MB external hard disk and GPS timing system. These were set on trigger mode to record local and distant earthquakes at 100 samples/sec. The digital stations were equipped with three component short period sensors – Mark products L4-3D (3 nos.) and SM3-KV seismometers (7 nos.) of the Institute of Physics of the Earth, Moscow. The frequency range for L4-3D sensors is 1 Hz to 25 Hz while that of SM3-KV sensors has flat velocity response from 0.5 Hz to 50 Hz. A typical earthquake recorded at station "MWD" is presented in figure 3.

Initially all the ten stations were operated in the Koyna-Western Ghat segment (30 km×50 km) and subsequently shifted along the Konkan coast and in the epicentral region of the 1967 earthquake to determine the detailed crustal structure of the region. Details of the location of seismic stations and the period of operation are provided in table 1.

4. Seismic trend

P and S arrival times for earthquakes recorded at a minimum of six stations in the network were used to compute hypocenters using HYPO71PC (Lee and Valdes 1985). With the availability of the GPS timing system, reliability of the internal clock systems was always better than a few microseconds. Reading accuracy for the arrival time of P and S phases is 0.01–0.03 sec and 0.05–0.10 sec. respectively. 1-D P-velocity model for depths > 1 km is adopted from Krishna *et al* (1989) whilst for depths < 1 km from

Table 2. *P-velocity model used to compute hypocenter parameters.*

Velocity model for Koyna region	
Depth (km)	P-Velocity (km/s)
0.00	2.90
0.30	4.70
1.00	6.25
2.50	6.30
8.00	6.35
12.00	6.40
20.50	6.49
30.00	6.79
40.00	8.20

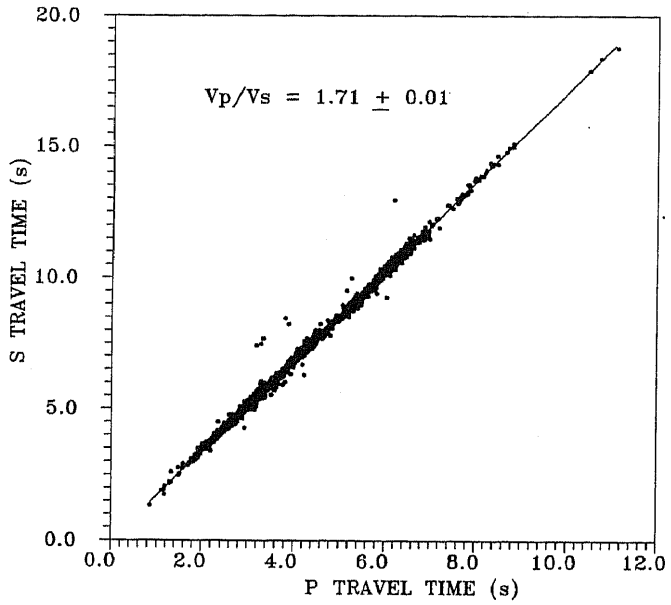

Figure 4. V_P/V_S ratio inferred from P- and S-wave travel time data.

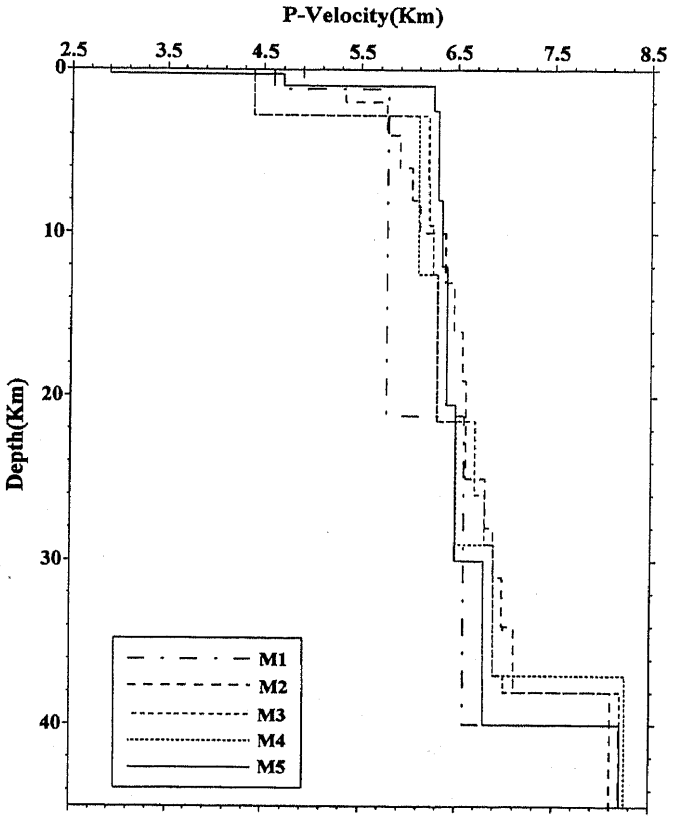

Figure 5. Different velocity models used to compute the locations and error statistics.

Athavale and Mohan (1976). This is presented in table 2. The model does not take into account any LVL. V_P/V_S ratio (1.71±0.01) has been computed from P- and S-wave travel time data (figure 4). The velocity model (M5) is found to be the most appropriate in locating earthquakes compared to four others (figure 5) as it produced least root mean square (RMS)

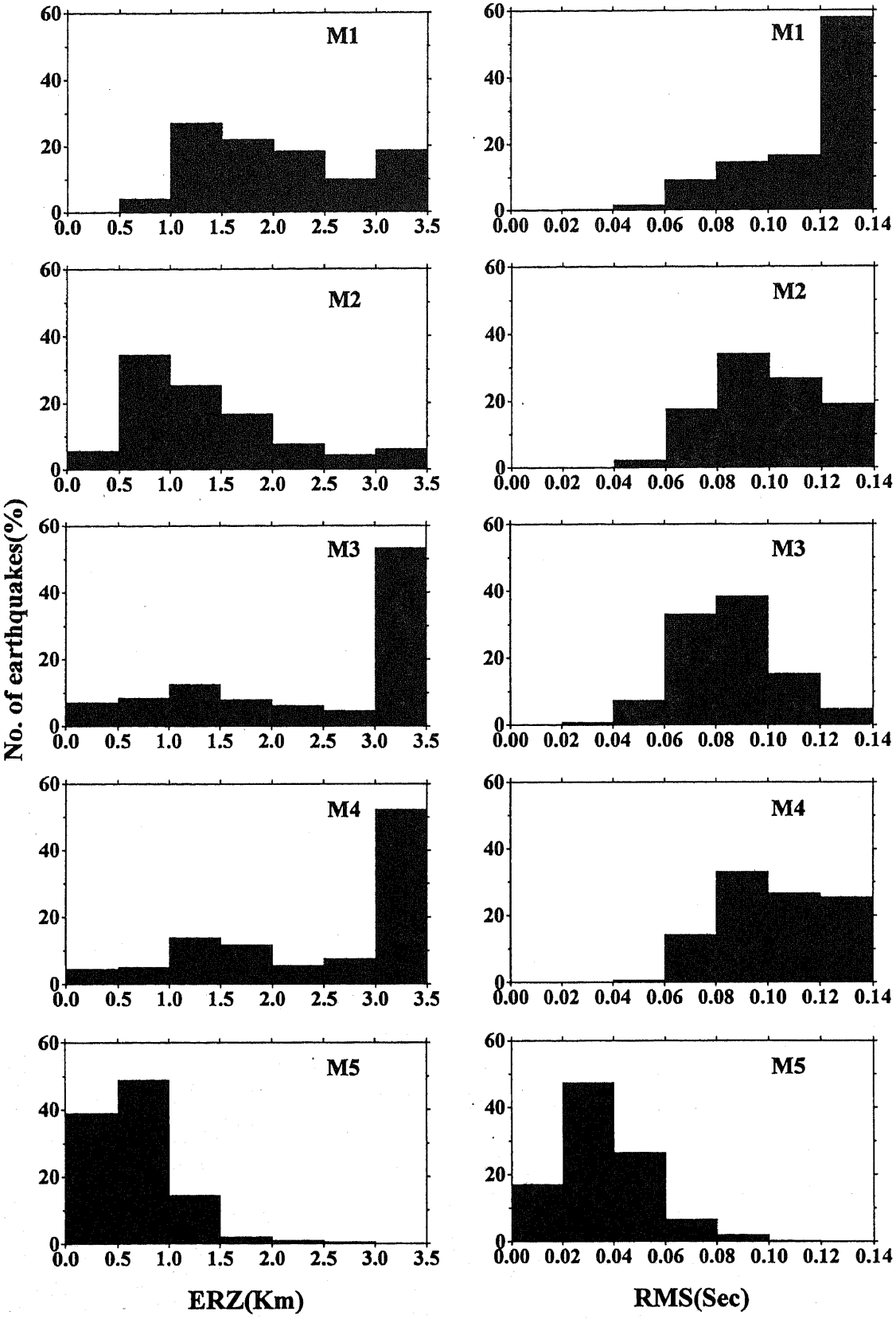

Figure 6. Comparison of RMS travel time residuals, errors in focal depth of 406 earthquakes for different velocity models. Note that the least errors are achieved for model M5 presented in table 2.

travel-time residuals and the error in focal depths (ERZ). The summary of statistical results is shown in figure 6.

The velocity model corresponds to a laterally homogeneous flat layered earth. To correct for lateral heterogeneity in seismic velocities and differences in

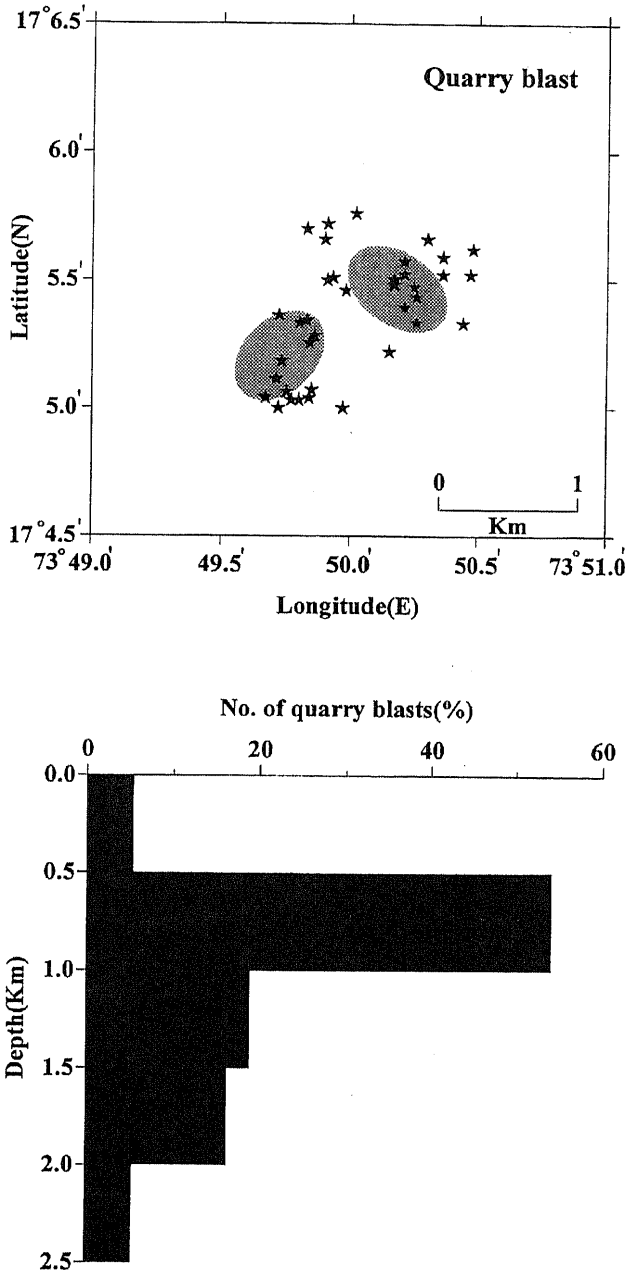

Figure 7. Locations and computed depth distribution of quarry blasts used for bauxite mining. Shaded areas show blasting sites.

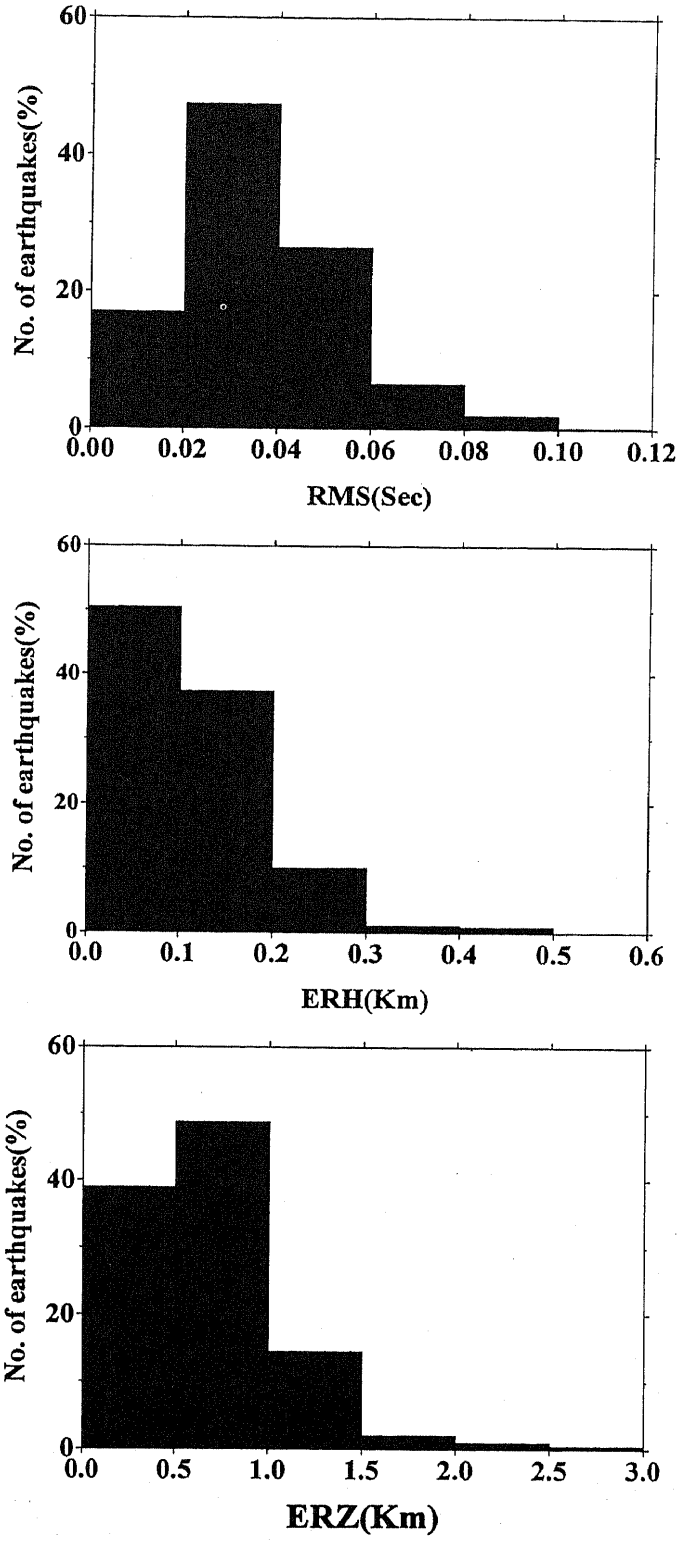

Figure 8. Error statistics for hypocenter parameters (RMS, ERH, ERZ) of 406 earthquakes for the velocity model (table 2) used in this study.

station elevations, initially the earthquakes were located without station delays. Subsequently, the median station delays obtained from the station residuals of the best events (A quality) were used to relocate earthquakes.

To establish the accuracy of earthquake hypocenters, we located a number of quarry blasts used for bauxite mining in an area of $2\times2\,\mathrm{km}^2$ centred around 17°5.50'N, 73°49.90'E (figure 7). Only P-wave arrival times were used in locating the blasts and the RMS residuals were found to be 0.06 sec or less. Comparing the observed and computed hypocenter parameters, we conclude that the epicentral error is generally less than 0.5 km while the error in focal depth estimation is less than 1.5 km (80% of blasts). As these blasts are located in a corner of the network and are surface focus in nature, the observed error bound would possibly represent the maximum. Using both P and S

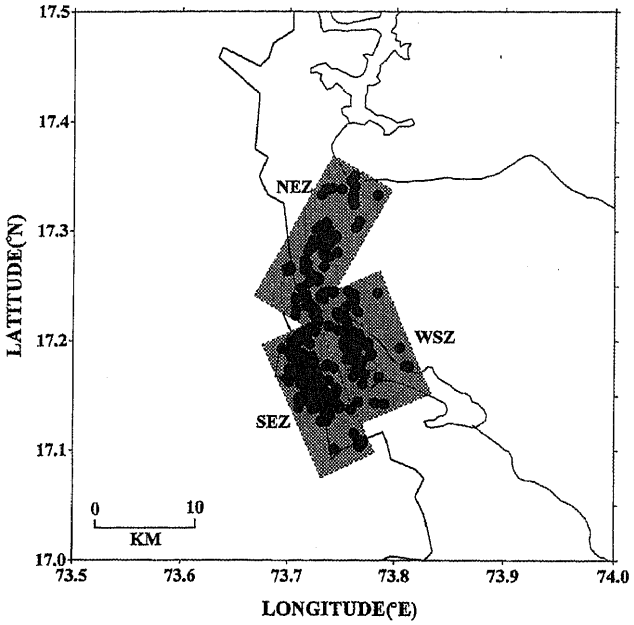

Figure 9. Seismicity pattern inferred from epicenter locations of 406 earthquakes (magnitude range:- $0.6 \leq M_d \leq 4.2$). Based on the seismic trend, three zones are identified as north escarpment zone (NEZ), southern escarpment zone (SEZ) and Warna seismic zone (WSZ).

data, we expect lower errors in hypocenter estimates for a typical earthquake at depth compared to blasts. Figure 8 presents error statistics of hypocentral parameters of earthquakes using the velocity model (M5).

Having assessed the reliability of hypocenter computation, we present the seismicity pattern in figure 9 using more than 400 earthquakes of quality A and B. The seismic zone shows a segmented pattern – starting as a single seismic tract in the north with a NE-SW trend, it branches into two distinct zones with NW-SE trend in its southern part. For the sake of identification and further analysis, these zones are named as NEZ (northern escarpment zone), SEZ (southern escarpment zone) and WSZ (Warna seismic zone). Hypocenters in each seismic zone are projected onto a vertical plane perpendicular to their epicentral trends (figure 10). The NEZ shows a dip ($\approx 45°$) in the NW direction while the other two segments SEZ and WSZ are near vertical.

For the entire KSZ as well as the individual segments, the earthquake frequency-depth distribution is presented in figure 11. In NEZ and WSZ, seismicity is confined to the depth levels 3 to 10 km whereas in SEZ it is largely restricted to 3 to 8 km. Seismicity is skewed in depth for NEZ and WSZ in contrast to a well-behaved pattern for SEZ. Considering the depth above which 90% of the events occur and the median depth of events, we observe a deepening of seismic activity of the order of 2 km in NEZ and WSZ compared with SEZ. Also, the depth of the peak seismic activity is about 2 km more in NEZ and WSZ (7 to 8 km) compared to SEZ (5 to 6 km). Shallower

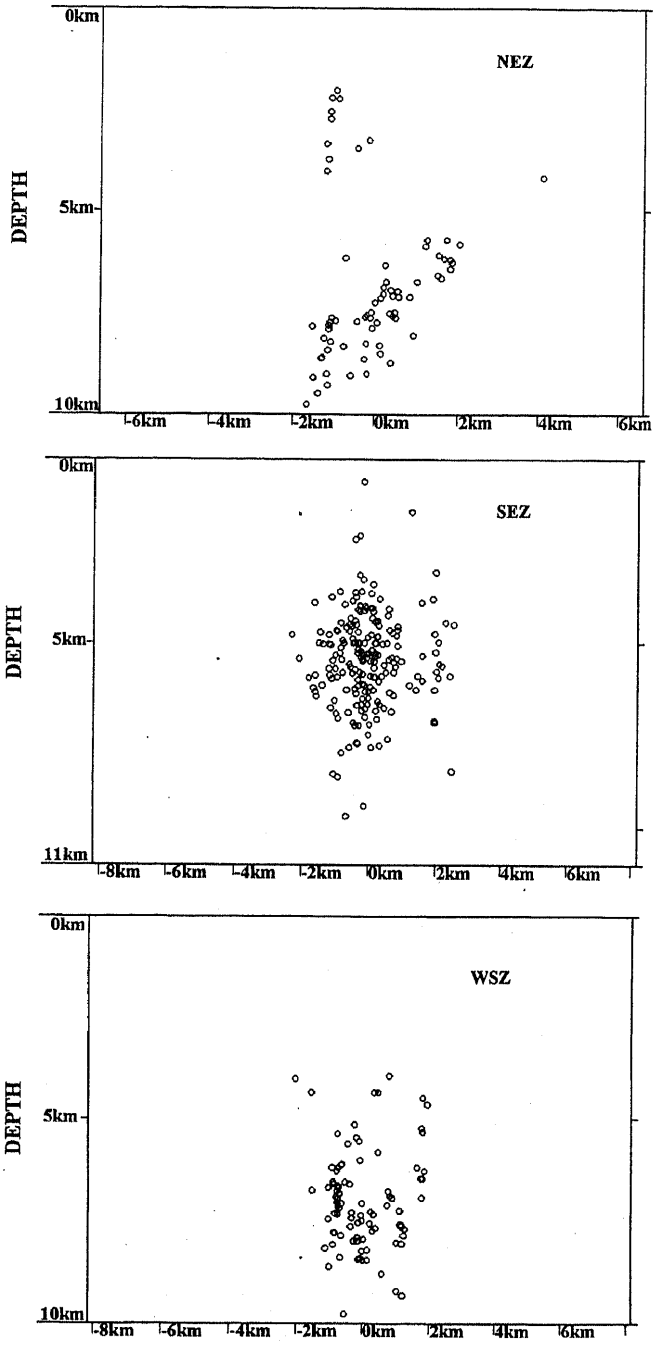

Figure 10. Depth sections for NEZ, SEZ and WSZ (hypocenters in each seismic zone are projected onto a vertical plane perpendicular to their epicentral trends).

events are absent in NEZ and WSZ while a few occur in SEZ. The earthquake depth distributions show similar behaviour for NEZ and WSZ and the two may be grouped into a single seismic zone. NEZ is well identified with the 1967 Koyna earthquake fissure zone. The WSZ shows a remarkable correlation with the earlier proposed steep Warna fault (Peshwa 1991) lying between Koyna and Warna rivers. The seismicity associated with Warna fault (WSZ) extends up to the Western Ghat escarpment zone. Talwani (1997) also made a similar observation.

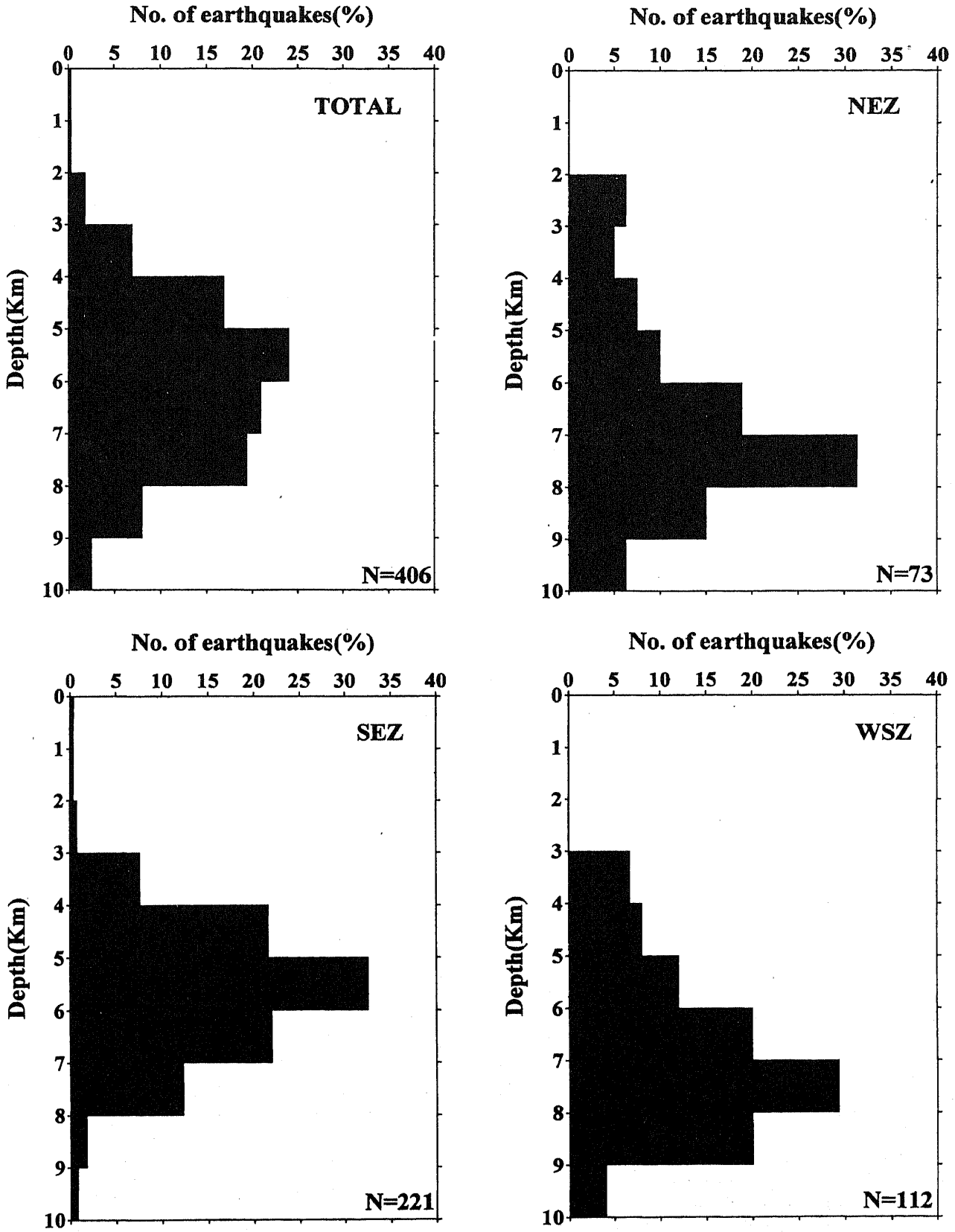

Figure 11. Earthquake frequency-depth distributions for entire KSZ as well as individual segments. The segment NEZ and WSZ show similar depth distribution.

Based on the above analysis of seismicity pattern with depth we infer a single causative fault system for NEZ and WSZ. This has an arcuate shape and lies between Koyna and Warna. In contrast, the SEZ follows the Western Ghat escarpment branching out from the NEZ-WSZ system. We critically examine the

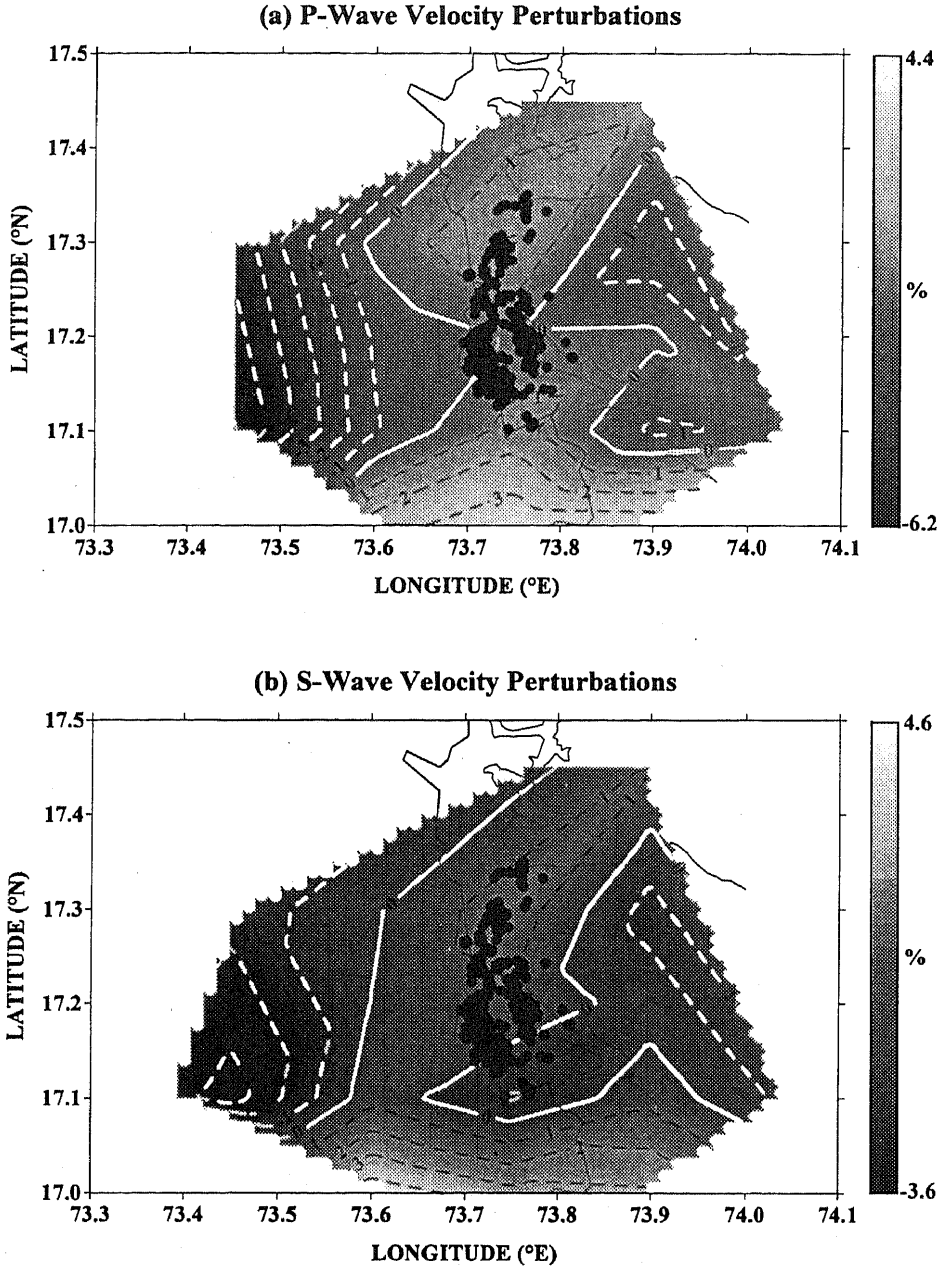

Figure 12. Velocity imaging of the seismogenic crust (0–10 km) in Koyna region using local earthquakes. (a) *P*-wave velocity perturbations (b) *S*-wave velocity perturbations.

cause for the difference in the depth distribution of earthquakes as well as their patterns observed in these two earthquake zones. Factors controlling the depth distribution of earthquakes include thermal structure, lithology, strain rate and stress level (Miller and Furlong 1988). Observed heat flow in the vicinity of the 1967 earthquake epicenter is $\approx 41\,\mathrm{mW/m^2}$ (near Alore, Koyna). We do not expect any major variation in heat flow within the study area, and therefore it is unlikely to be a controlling factor in the observed variation in the depth of seismicity. Also, these two seismic zones being interwoven and confined within the same geological terrain, a drastic variation in lithology and its control on the variation in the depth of seismicity is not favoured. Assuming that the strain rate is nearly the same in both the fault systems, we argue in favour of a low level of stress on SEZ, as the possible cause for shallower seismic activity. A quantitative estimation requires detailed numerical simulation.

The upper cut off in seismicity has been generally attributed to the transition from stable (velocity strengthening within shallow unconsolidated gouge) to unstable frictional sliding (velocity weakening in the consolidated material below) (Scholz 1998). Based on the observation of velocity strengthening (aseismic slip) in unconsolidated gouge together with stability analysis Marone and Scholz (1988) and Marone (1998) predicted that earthquakes do not nucleate within the upper region of a mature fault. From the seismicity

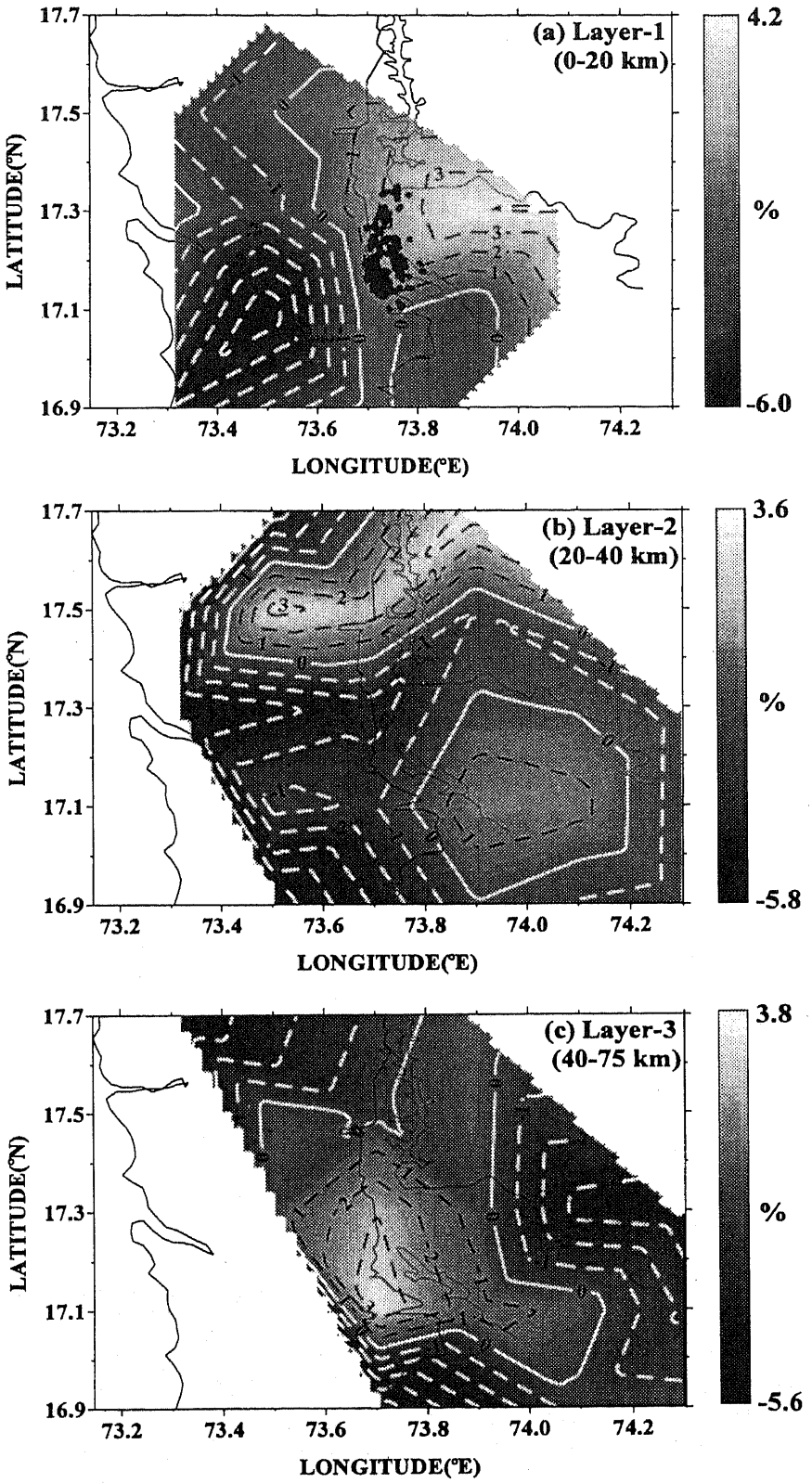

Figure 13. *P*-wave velocity image of crust and uppermost mantle beneath KSZ using teleseismic travel times at depth levels (a) 0–20 km; (b) 20–40 km; (c) 40–75 km.

data, one can infer the depth of the upper stability transition and further the depth of unconsolidated fault gouge. In the KSZ, this is observed to be up to a depth of 3–4 km, as 90% of the seismic activity is confined below 4 km. The absence of seismicity at shallower depths in the KSZ therefore indicates the presence of a mature fault system with well-developed gouge zone.

5. Velocity imaging of the seismic zone: Local earthquake and teleseismic tomography

Seismic patterns provide a direct means to identify a seismogenic fault and its lateral as well as vertical extent. However, physical property of the fault zone and its variations, which may provide a clue to the seismogenesis in the region remain to be resolved. Seismic velocity in crustal rocks depends on factors such as the temperature, presence of fluids, pore fluid pressure and composition. Therefore, 3-D velocity imaging of the seismogenic crust using local earthquake travel time data should be successful in resolving the physical properties of seismically active faults. Results from earlier seismic tomography studies of seismically active source regions show that high velocity regions represent competent parts of the fault zone (Lees 1990; Lees and Nicholson 1993; Zhao and Kanamori 1995) while the low velocity regions represent over-pressured fluids (Eberhart-Phillips *et al* 1995; Zhao *et al* 1996).

To describe the source zone behaviour and processes, we present a 3-D V_P and V_S image of the seismogenic crust. We used the tomographic method developed by Zhao *et al* (1992) to determine 3-D P- and S-wave velocity structure using local earthquake arrival time data. The seismogenic crust is represented as a single layer up to 10 km, with a horizontal grid spacing of 5 km. The resulting velocity image is presented in figure 12. Reliability of velocity anomalies has been tested through checkerboard resolution test (Zhao *et al* 1992). Both P- and S-wave velocity tomographic inversion show a lateral variation of about 4% with, 1% to 2% higher velocity observed in the seismogenic zone compared to 2% to 3% lower velocity in the adjoining regions.

To further probe the depth extent of high velocity and its lateral extent we examined P-wave velocity image of deeper zones (crust and uppermost mantle) using teleseisms from distance range 30°–90°. The detailed description of methodology can be found in Iyer and Hirahara (1993). This network configuration constrains to depth resolutions at 20, 40 and 75 km with horizontal gridding at 10 km. Checkerboard analysis indicates poor ray coverage and resolution at lower crustal level (20–40 km). The P-wave velocity image (figure 13) shows that the high velocity beneath the seismic zone resolved through local earthquake data continues further down to depths of up to 70 km into the uppermost mantle. The lower end of this depth range could not be resolved.

Two major competing hypotheses put forward for seismogenesis, include pore-fluid pressure (Raleigh 1971) and lithological compaction (Zhao and Kanamori 1995). Various mechanisms have been suggested for producing high pore pressure in fluid-saturated rocks, for example, tectonic compression (Fertl 1976), porosity reduction by precipitation of minerals (Levorsen 1954) and mineral reactions that release water (Burst 1969). Christensen (1989) studied the seismic velocity structure of the earth's crust in relation to the role played by high pore pressure. He observed that P- and S-wave velocities measured at carefully controlled confining and pore pressures show significant decrease with increasing pore pressure. The observed high P- and S-wave velocity beneath the KSZ argue against the presence of a high pore fluid pressure zone. The correlation of high P- and S-wave velocity and seismic activity probably implies that the earthquakes in the KSZ occur in a more competent zone having a strong lithologic control extending to deep crust/uppermost mantle. This deep structural feature is also evidenced from residual positive (+10 mgal) Bouguer gravity anomaly over the seismic zone (Subba Rao, D.V., in preparation). Such a geological inhomogeneity facilitates strain accumulation under the action of ambient tectonic forces.

6. Conclusion

The Koyna seismic tomography digital network of 20 stations was operated for 20 months (April 1996–Dec. 1997) in a leap frog manner with atleast 50% overlap of recording stations. Local, regional and teleseismic events were recorded by 24 bit REFTEK/PASSCAL digital recorders equipped with short period triaxial seismometers and GPS timing system. Local earthquakes recorded by atleast six stations were used for mapping the seismogenic faults and upper crustal velocity structure. Statistical analysis reveals well-constrained epicenters and focal depths estimate. More than 400 earthquakes of A and B quality show spatial clustering with well defined segmentation. Using epicenters and depth distributions of earthquakes, we could delineate the seismogenic faults. An arcuate shape seismogenic zone lies between Koyna and Warna while a NW-SE trending zone branches out from it and follows the Western Ghat escarpment. Both the fault systems lack shallow seismicity within the first 3 km. We interpret this behaviour as arising from the presence of a mature fault with well developed gouge zones which inhibit nucleation of earthquakes at shallower levels. The base of the seismogenic zone is at a depth of about 10 km.

3-D velocity imaging of the seismogenic crust (0–10 km) using local earthquake travel time data shows P- and S-wave velocity variations up to 4% where the seismic zone has $\approx$ 2% higher velocity compared with $\approx$ 2% to 3% lower velocity in the surrounding region. The high velocity observed beneath the seismic zone is inferred to have deep crustal and probably uppermost mantle root. We interpret the higher velocity observed beneath the KSZ as representing the stronger, more competent material defining major asperities where

stress is concentrated and earthquakes tend to nucleate.

These preliminary results await detailed analysis and modelling from the larger data set acquired by the network.

Acknowledgements

We are grateful to Prof. Vinod K Gaur and Prof. K S Valdiya for sparing innumerable hours in discussion, guidance and encouragement. This research project is supported by Deep Continental Studies Program of the Department of Science and Technology. We have benefited by discussions with several individuals. In particular, we are grateful to Dr. T M Mahadevan, Prof. D Mukhopadhyay, Prof. Pradeep Talwani, Dr. Upendra Raval and Dr. D N Awasthi. Dr. K R Gupta provided the necessary impetus to the program. We deeply acknowledge his contribution. The study would not have been feasible without the support of the Warna Dam project authority. We are grateful to our colleagues Dr. D S Ramesh and M S Kumar for their contributions to the field program.

References

Athavale R N and Mohan I 1976 Integrated geophysical studies in the Koyna Hydro-electric project area of Maharashtra state, India; *Technical Report, NGRI*

Burst J F 1969 Diagenesis of Gulf Coast clay sediments and its possible relation to petroleum; *American Association of Petroleum Geologists Bulletin* **53** 73–93

Chadha R K, Gupta H K (and 10 others) 1997 Delineation of active faults, nucleation process and pore pressure measurements at Koyna, (India); *Pure Appl. Geophys.* **150** 552–562

Christensen I N 1989 Pore pressure, seismic velocities and crustal structure, in Pakiser L C and Mooney W D, Geophysical framework of the continental United States: Boulder, Colorado; *The Geological Society of American Memoir* **172** 783–798

Dziewonski A M, Ekstrom G, Franzen J E and Woodhouse J H 1988 Global seismicity of 1980; Centroid moment tensor solutions for 515 earthquakes; *Phys. Earth Planet. Int.* **50** 127–154

Eberhart-Phillips D, Stanley W D, Rodriguez B D and Lutter W J 1995 Surface seismic and electrical methods to detect fluid related to faulting; *J. Geophys. Res.* **100** 12919–12936

Fertl W H 1976 Abnormal formation pressure (New York, Elsevier) 382

Geological Survey of India, 1968, A geological report on the Koyna earthquake of 11th Dec. 1967, Satara District, Maharastra State, Unpublished Report (GSI), p. 242

Gubin I E 1968 Seismic zoning of Indian peninsula; *Bull. Int. Inst. Seism. Earthquake Engg.* **5** 109–139

Gubin I E 1969 Seismic zoning of the western margin of the Indian peninsula in Maharashtra state, UNESCO, serial no.1519/BMS.RD/SCE, Paris

Gupta H K, Narain H, Rastogi B K and Mohan I 1969 A study of the Koyna earthquake of Dec. 10, 1967; *Bull. Seism. Soc. Am.* **70** 1149–1162

Gupta H K 1992 Reservoir Induced Earthquakes (Amsterdam: Elsevier Publishers) p. 364

Iyer H M and Hirahara K 1993 Seismic Tomography: Theory and Practice, (Chapman and Hall) 319–360

Kelkar Y N 1968 Earthquakes experienced by Maharashtra in the past three hundred years, Kesari (Marathi Language Daily), Jan. 7, p. 7, Pune

Krishna V G, Kaila K L and Reddy P R 1989 Synthetic seismogram modeling of crustal seismic record sections from the Koyna DSS Profiles in Western India. In: *Properties and process of the Earths Lower crust; Am. Geophys. Union Geophys. Monogr.* **51** IUGG 6, 143–157

Langston C A 1981 Source inversion of seismic waveform: The Koyna India earthquake of Sept. 13, 1967; *Bull. Seism. Soc. Am.* **71** 1–24

Langston C A and Franco-Spera M 1985 Modeling of Koyna, India, aftershock of 12th Dec. 1967; *Bull. Seism. Soc. Am.* **75** 651–660

Lee W H K and Raleigh C B 1969 Fault plane solution of the Koyna (India) earthquake; *Nature* **223** 172–173

Lee W H K and Valdes C M 1985 HYPO71PC: A personal computer version of the HYPO71 earthquake location program; *U. S. Geol. Surv. Open-File Report* 85–749 p. 43

Lees J M 1990 Tomographic *P*-wave velocity images of the Loma Prieta earthquake asperity; *Geophys. Res. Lett.* **17** 1433–1436

Lees J M and Nicholson C E 1993 Three dimensional tomography of the 1992 southern California earthquake sequence: constraints on dynamic earthquake rupture? *Geology* **21** 387–390

Levorsen A I 1954 *Geology of petroleum* (San Francisco: W H Freeman) p. 703

Mahadevan T M 1994 Deep continental structure of India: A review; *Geol. Soc. India Mem.* **28** p. 569

Mandal P, Rastogi B K and Sarma C S P 1998 Source parameters of Koyna earthquakes, India; *Bull. Seism. Soc. Am.* **88** 833–842

Marone C 1998 Laboratory derived friction laws and their application to seismic faulting; *Ann. Rev. Earth Planet. Sci.* **26** 663–696

Marone C and Scholz C H 1988 The depth of seismic faulting and the upper transition from stable to unstable slip regimes; *Geophys. Res. Lett.* **15** 621–624

Miller C K and Furlong K P 1988 Thermal-mechanical controls on seismicity depth distribution in the San Andreas fault zone; *Geophys. Res. Lett.* **15** 1429–1432

Pascoe E H 1964 A manual of the Geology of India and Burma; (Calcutta: Govt. of India Press)

Peshwa V V 1991 Geological studies of Chandoli dam site area Warna Valley, Sangli Dist. Maharashtra State, Studies based on remote sensing techniques; Unpublished report to Maharashtra Engg. Res. Inst., Nasik, Dept. of Geology, Pune Univ., p. 45

Raleigh C B 1971 Earthquake control at Rangely, Colorado: EOS Transactions of the American Geophysical Union, **52** p. 344

Scholz C H 1998 Earthquakes and friction Laws; *Nature* **391** 37–42

Snow D T 1982 Hydrology of induced seismicity and tectonism: Case history of Kariba and Koyna; *Geol. Soc. Am. Spl. Paper* **189** 317–360

Talwani P, Kumar Swamy S V and Sawalwade C B 1996 The revaluation of seismicity data in the Koyna-Warna Area, 1963–1995; *Univ. of South Carolina, Tech. Rep.* p. 343

Talwani P 1997 Seismotectonics of the Koyna-Warna Area, India; *Pure. Appl. Geophys.* **150** 511–550

Valdiya K S 1984 Aspects of Tectonics: Focus on South-Central Asia, (New Delhi: Tata McGraw-Hill)

Widdowson M and Cox K G 1996 Uplift and erosional history of the Deccan Traps, India: Evidence from laterites and drainage patterns of the Western Ghats and Konkan Coast; *Earth Planet. Sci. Lett.* **137** 57–68

Zhao D, Hasegawa A and Horiuchi S 1992 Tomographic imaging of *P*- and *S*-wave velocity structure beneath northeastern Japan; *J. Geophys. Res.* **97** 19909–19928

Zhao D and Kanamori H 1995 The 1994 Northridge earthquake: 3-D crustal structure in the rupture zone and its relation to the aftershock locations and mechanisms; *Geophys. Res. Lett.* **22** 763–766

Zhao D, Kanamori H, Negishi H and Wiens D 1996 Tomography of source area of the Kobe earthquake: Evidence for fluids at the hypocenter?; *Science* **274** 1891–1894

MS received 8 September 1998; revised 22 February 1999